Cancer Immunology, Immunotherapy (2021) 70:1877–1891
https://doi.org/10.1007/s00262-020-02808-0

ORIGINAL ARTICLE

Transcriptional regulation of VEGFA expression in T-regulatory cells from breast cancer patients

Kirti Kajal[1] · Sayantan Bose[1] · Abir K. Panda[1] · Dwaipayan Chakraborty[1] · Sreeparna Chakraborty[1] · Subhadip Pati[1] · Tania Sarkar[1] · Subhanki Dhar[1] · Dia Roy[1] · Shilpi Saha[1] · Gaurisankar Sa[1]

Received: 19 July 2019 / Accepted: 21 November 2020 / Published online: 4 January 2021

Abstract

The initiation of new blood vessel formation (neo-angiogenesis) is one of the primary requirements for the establishment of tumor. As the tumor grows beyond a certain size, a hypoxic-condition arises in the inner core of tumor, triggering the release of chemokines, which attract T-regulatory (Treg) cells in the tumor-site. The presence of FOXP3, a lineage-specific transcription factor, expressing Treg cells in various types of tumor implements immunosuppressive and tumor-promoting strategies. One such strategy is the invitation of endothelial cells for neo-vascularization in the tumor site. Here we report that as the disease progresses, Treg cells from breast cancer patients are capable of secreting high-amount of VEGFA. The VEGFA promoter lacks Treg-specific transcription factor FOXP3 binding site. FOXP3 in association with locus-specific transcription factor STAT3 binds to VEGFA promoter to induce its transcription in Treg cells obtained from breast cancer patients. Treg cell-secreted VEGFA induces neo-angiogenesis from endothelial cells under in-vitro conditions. Targeting Tregs in mice with breast tumor reduces tumor growth as well as the level of neo-angiogenesis in the tumor tissue.

Keywords Endothelial cell · FOXP3 · Treg cells · STAT3 · VEGFA · Neo-angiogenesis

Abbreviations

CAM	Chorioallantoic membrane
EGF	Epidermal growth factor
FGF	Fibroblast growth factor
HUVEC	Human umbilical vein endothelial cells
tSNE	T-distributed Stochastic Neighbour End-Joining
VEGFR2	Vascular endothelial growth factor receptor-2

Introduction

T lymphocytes play a significant role in protecting our body against foreign pathogen and maintain immune homeostasis. Naïve $CD4^+$ T cells differentiate into two types based on responsive signals they receive after activation, which includes the effector (Th1, Th2, and Th17) and T-regulatory (Treg) cells [1]. Treg cells are developed either in the thymus (nTreg) or peripheral circulation (iTreg) and are immune-suppressive [1, 2]. Treg cells suppress self-reactive T-cells in the periphery; induce peripheral tolerance, regulate the immune response to self-antigen, quasi-self (antigen expressed by tumor cells) and non-self (small microorganisms and allografts) and promote self-tolerance [3]. These suppressor cells are characterized by the expression of CD4, CD25, lineage-specific X-chromosome-linked transcription factor FOXP3, and lower expression of CD127 [4, 5]. Tumor microenvironment comprises of nearly 30% of tumor cells while rest being cancer-associated fibroblasts, stromal cells, pericytes, endothelial cells, adipocytes, immune cells like natural killer cells, macrophages, T-cells, B-cells, dendritic cells, neutrophils, platelets and suppressive cells like Treg cells and myeloid-derived suppressor cells (MDSCs), etc. [6, 7].

Kirti Kajal and Sayantan Bose contributed equally.

Supplementary Information The online version contains supplementary material available at https://doi.org/10.1007/s00262-020-02808-0.

✉ Gaurisankar Sa
gauri@jcbose.ac.in

[1] Division of Molecular Medicine, Bose Institute, P-1/12, Calcutta Improvement Trust Scheme VII M, Kolkata 700 054, India

Angiogenesis, in general, refers to formation of new blood vessels that occurs during several physiological processes like foetal development, wound healing, pregnancy, menstrual cycle etc. Angiogenesis involves a set of events regulated by different molecular determinants that leads to formation of new blood vessels causing neo-vascularisation [8, 9]. Judah Folkman first reported that new blood vessel formation takes place in solid tumor [10]. The inability of blood vessels to reach the core of the fast and continuous growing tumor generates central hypoxia. Central hypoxia completely transforms the normal microenvironment of the diseased organ [11]. In hypoxic-condition tumor cells, secrete CCL28 chemokine to attract $CCR10^+$ Treg cells to the tumor site [12]. Increased infiltrated Treg cells are related to poor prognosis in many tumors like mammary, ovarian, gastric, prostrate, pancreatic, lung, etc. [13–17]. At the escape-stage of tumor immune evasion, Treg cells suppress the host's immune system and facilitate tumor progression [18]. Treg cells facilitate tumor progression by (a) releasing immunosuppressive cytokines such as IL10, TGFβ, IL35, etc., (b) killing T-effector cells, (c) altering immunogenic to tolerogenic micro-environment and (d) suppression of antigen presenting cells viz. dendritic cells [19, 20].

Angiogenesis depends on the balance between pro-and anti-angiogenic signals. Increase of tumor size leads to impaired supply of nutrients and oxygen to the core of the outgrowth which prompts pro-angiogenic signals that switch on the angiogenesis process. This process leads to increased secretion of cytokines and chemokines like vascular endothelial growth factor-A (VEGFA), bFGF, EGF [21]. Induction of angiogenesis is an established hallmark of cancer [22]. In tumor microenvironment, immune cells are known to modulate the 'angiogenic switch' and in ovarian cancer Treg cells have been reported to release substantial amounts of VEGFA and promote endothelial cell proliferation [23]. The VEGFA binds to VEGF receptor-2 (VEGFR2; Flk-1/KDR) present over the surface of endothelial cells. These phenomenon promotes endothelial cell proliferation and migration required for neo-vascularization through the activation of receptor tyrosine kinase and its down-stream signalling molecules [24, 25].

Treg cells produce a high level of VEGFA in hypoxic conditions, but there are few questions, which remain unanswered: (1) whether Treg cells produce sufficient VEGFA, that can trigger neo-angiogenesis and (2) what are the mechanisms of transcription of *VEGFA* gene in Treg cells. Here we report that since *VEGFA* promoter lacks FOXP3-binding sites, FOXP3 and STAT3 cooperatively occupy *VEGFA* promoter to induce *VEGFA* transcription in Treg cells. The resultant secretion of VEGFA by Treg cells can promote neo-angiogenesis from endothelial (HUVEC) cells.

Materials and methods

Human breast tissue and blood sample

Twenty-four age/sex-matched female healthy volunteers and 24 female patients with breast cancer were recruited into the study (patient details provided in Supplementary Table 1). The study was performed by collecting human tissues and blood samples from different grades of breast cancer patients.

Cell isolation and culture

Peripheral blood collected from healthy volunteers and breast tumor patients was centrifuged over lymphocyte separation medium (Histopaque, Sigma) to obtain total leucocytes. Cells obtained were counted under a microscope using a haemocytometer. $CD4^+CD25^+CD127^-$ Treg cells were isolated from total leucocytes with the combination of biotinylated CD127 antibody and BD IMag™ Treg isolation kit (BD Biosciences). $CD4^+CD25^-$ effector T-cells and $CD4^+CD45RA^+$ naïve cells were also sorted from peripheral blood of healthy individuals using combinations of magnetic bead tagged antibodies by the BD IMag™ system. For activation of effector T-cells, where necessary, the cells were cultured in anti-CD3 and anti-CD28 antibody coated plate containing complete RPMI-1640 medium at 37 °C in a humidified incubator containing 5% CO_2 for 72 h. Treg cells were kept in RPMI-1640 medium supplemented with 10 ng/ml IL2. 1×10^6 MCF-7 cells were seeded in a T-75 tissue culture flask and conditioned media from 72 h cultured cells were collected and centrifuged at 1000 rpm for 5 min to precipitate floating cells. Cell free supernatants were collected and stored at – 80 °C. To mimic conditions of the tumor micro-environment, effector/naïve T-cells/Treg cells were cultured with a 1:1 mixture of fresh media and the cancer cell-free supernatant. Human umbilical vein endothelial cells were cultured in HUVEC growth supplemented media (HiMedia) supplemented with 5% heat-inactivated FBS (Lonza, USA) in the presence of penicillin, streptomycin and amphotericin B. Cells were cultured in 5% CO_2 at 37 °C. All cells were periodically checked for mycoplasma contamination using MycoFluor™ Mycoplasma Detection Kit (ThermoFisher Scientific).

Animal model

Mice mammary epithelial cancer 4T1 cells (2×10^6) were inoculated in the mammary fat-pad of syngenic BALB/c mice. Mice were divided into four groups with five mice in each set: (1) 1 week, (2) 2 weeks, (3) 3 weeks, and (4)

4 weeks. Mice were kept under observation for 28 days. Every alternate day tumor volume was measured. After 28 days, mice were sacrificed. Images of mice were taken before and after sacrifice. Weight and volume of tumor tissues were measured after sacrifice. For the immunohistochemistry study, tumor tissues were fixed in bouin's solution.

For over-expression/knockdown of Foxp3 in mice, 1×10^6 transducing units of respective lentivirus/retrovirus particles mixed with polybrene (8 µg/ml) were injected into the tail vein of mice bearing 4T1 tumors twice a week. After 24 days mice were sacrificed and tumor tissues were harvested. Single cell suspensions were obtained by digesting the tissue with 1 mg/ml treatment for 2 h and passing through nylon mesh and used for detection of $CD4^+CD25^+Foxp3^+$ Tregs and $CD31^+$ cells by flow cytometry. Micro-sections of the tissues were also prepared for immunofluoresence detection of CD31.

Preparation of lentivirus/retrovirus for Foxp3 knockdown/over-expression

For Foxp3 knock-down in mice, shRNA clones in pLKO.1 lentiviral vector targeted against mouse Foxp3 gene were used (GPP clone IDs: TRCN0000071987, TRCN0000413282). The packaging of lentiviruses was performed by in HEK 293T cells by co-transfection with gag/pol packaging plasmid psPAX2 (kind gift from Didier Trono; Addgene plasmid #12260), µg pLKO.1-shRNA vectors, envelope plasmid pMD2.G (kind gift from Didier Trono; Addgene plasmid #12259) by the calcium phosphate precipitation method using Profection mammalian transfection system purchased from Promega (CA, USA). Thereafter the medium was replaced with fully supplemented DMEM and supernatant collected after 24 and 48 h. Cell debris was removed by centrifugation at 1500 rpm for 5 min at 4 °C, followed by passage through a 0.45 µm pore PES filter. For concentration Polyethylene-glycol (PEG-8000) solution in 1X PBS was mixed with 20 ml of supernatant to a final concentration of 12% and kept overnight at 4 °C and centrifuged at 4000 rpm for 20 min. Pelleted viruses were resuspended in serum and antibiotic free DMEM. Aliquots were stored at − 80 °C.

For Foxp3 ectopic over-expression in mice, MIGR mFOXP3 plasmid (kind gift from Dan Littman; Addgene plasmid #24067) was used. Packaging of retroviruses was performed in HEK 293T cells by co-transfection with gag/pol (kind gift from Tannishtha Reya; Addgene plasmid #14887), MIGR mFOXP3 and VSV.G (kind gift from Tannishtha Reya Addgene plasmid #148880). Transfection of cells and purification of retroviruses from media were performed in a similar process as mentioned for lentiviruses.

Flow-cytometry and ELISA

Breast cancer tissue was collected from patients undergoing surgical procedures to remove solid tumor mass. Single cells were prepared after collagenase (1 mg/ml) treatment for 4 h and passing through a nylon mesh. To analyze intracellular VEGFA level, cells were stimulated with PMA (10 ng/ml), ionomycin (1 µM) and Brefeldin A (10 µg/ml) (Sigma-Aldrich, St. Louis, MO). To analyze Treg cells in human breast tissue and blood samples, cells were fixed, permeabilized and labelled with V450/FITC-anti-CD4, PE/PE-Cy7-anti-CD25 and Alexa Fluor-647-anti-FOXP3 (BD Biosciences) and FITC-anti-VEGFA (Santa Cruz, CA) antibodies. Cells were analyzed in FACS Verse flow cytometer using FACS Suite software (BD Biosciences). For tSNE analysis, the steps outlined in the online documentation for FlowJo v.10 was followed [26]. The lymphocyte population was gated, and the $CD4^+$ population was subsequently marked. Additional gates were drawn on $CD4^+$ population signifying $CD4^+CD25^+$, $CD4^+FOXP3^+$, $CD4^+VEGFA^+$, $CD4^+CD127^+$ populations. A down-sample with ~ 2000 cells was performed on the $CD4^+$ populations from different grade tumor tissues, and the samples were concatenated. Dimensionality reduction (tSNE) was performed with the concatenated population creating the tSNE parameters. The $CD4^+$ population was displayed as a background contour plot, and the other sub-populations (CD25, FOXP3, and VEGFA) were overlaid on it. Appropriate query gates were drawn based on desired marker expressions. VEGFA in Human breast cancer patients serum, T-cells, and Treg cells spent media were measured by ELISA (Ray Biotech).

Transfection, qPCR and ChIP assays

T cell transduction was done with lenti viral FOXP3/STAT3/control-shRNA (Open Biosystem) using transduction facilitator hexadimethrine bromide (Sigma). Expression of *VEGFA*-mRNA was quantified by qPCR (forward primer 5′-TTGGAAACCAGCAGAAAGAG-3′ reverse primer 5′-CCAAAAGCAGGTCACTCACT-3′). ChIP assays were performed following the protocol from the ChIP assay kit (Millipore). To cross link the protein–DNA complexes, two million cells were fixed in 1% HCHO, 10 min at 37 °C. These cells were harvested, lysed in lysis buffer and incubated for 10 min on ice. To obtain DNA length between 200 and 1000 bp, cell lysates were sonicated, and then these cells were centrifuged at 13,000 rpm for 10 min at 4 °C. Cell supernatant obtained were incubated with FOXP3 (Santa Cruz, CA), p-STAT3 and Ac-H3 (Cell Signalling, USA) antibodies. Antibody-protein-DNA complexes were purified with protein A-agarose. Chromatin complexes were reverse cross-linked at 65 °C, and DNA was recovered [27]. By digesting proteins with 10 mg/ml proteinase K, DNA was

recovered. DNA fragments were amplified by PCR using specific primers. A ChIP-re-ChIP assay was performed by immunoprecipitating first-round of immunoprecipitates with a second antibody. DNA fragments were amplified by qPCR at STAT-binding site of VEGFA promoter using forward (5′-CTGGCCTGCAGACATCAAAGTGG-3′) reverse (5′-CTTCCCGTTCTCAGCTCCACAC-3′) primers.

Wound-healing and Sprout formation assay

The wound-healing assay was performed to observe the migration of human umbilical vein endothelial cells (HUVECs). Twelve well plates were coated with 0.5% gelatin. Cells were plated in gelatin coated plate and allowed to grow up to full confluence. These cells were serum starved, and the wound was created using sterile microtip. The cells were treated with rVEGF (10 ng/ml), T-cell, and Treg cell spent media (± anti-VEGFA). After 18 h of incubation, images were captured using an inverted phase-contrast microscope (Olympus IX71). The migration of cells to the wounded area was calculated using Image-J software. [28, 29]. For sprout formation assay, HUVEC has seeded on matrigel-coated (20 mg/ml) plates for 1 h at 37 °C. Cells were treated as mentioned above, and the formation of spontaneous vessel-like structures was imaged after 4–6 h under an inverted phase-contrast microscope. Tube forming complete network was counted [28, 30].

Chorio-allantoic membrane (CAM) assay

Chorio-allantoic membrane assay was performed using a 3-day-old fertilized egg under completely sterile conditions. Eggs were broken carefully in petridish to keep the embryo intact. VEFG/cell supernatants were added over filter paper. The filter paper was placed carefully over blood vessels; eggs were incubated at five $\%CO_2$, 37 °C. The eggs were monitored at a regular interval, and images were taken. Angioquant software was used to quantify images (http://www.cs.tut.fi/sgn/csb/angioquant/) [28, 31].

Confocal microscopy

T cells and Treg cells plated on poly-*l*-lysine-coated slides were fixed using 4% *p*-formaldehyde, permeabilized, and blocked with 3% BSA. To visualize FOXP3/VEGFA/p-STAT3 (Cell-signalling) cells were stained with specific antibodies counterstained with fluorochrome-conjugated secondary antibodies (Invitrogen). Nuclei were labelled with DAPI (4,6-diamidino-2-phenylindole). Stained cells were mounted with DPX. Images were captured under a Leica confocal microscope using 63 ×/100 × objectives. During imaging sessions, laser intensities and detector gains were maintained at the same level. Image analysis between pixels of different channels has been done using Image-J software [32].

Co-immunoprecipitation and western blot

The co-immunoprecipitation technique was employed to study the interaction between two proteins FOXP3 and STAT3. Cells were harvested and lysed in IP buffer (50 mM Hepes, pH 7.6, 150 mM NaCl, 1 mM EDTA, 1% Nonidet P-40, and 25% sodium deoxycholate) containing protease and phosphatase inhibitor cocktails. A total of 200 µg protein was used. Immunocomplexes were purified using anti-FOXP3 antibody and protein A/G-Sepharose beads (Invitrogen, USA). The immunopurified protein was immunoblotted with the anti-FOXP3/p-STAT3 antibodies [19, 33].

Immunofluoresence of tissue sections

Paraffin-embedded sections of breast tumor tissue were rehydrated with consecutively increasing gradients of ethanol. Heat-induced epitope retrieval was performed in sodium citrate buffer (10 mM sodium citrate, 0.05% Tween 20, pH 6.0). Tissue sections were blocked in blocking buffer (1% BSA and 0.05% Tween 20) for 30 min. To detect $CD4^+FOXP3^+$ cells, tissue sections were incubated overnight with α-CD4 and α-FOXP3 primary antibodies (Santa Cruz Biotechnology Inc.). For detection, Alexa-488 α-rat (for CD4) and Alexa-546 α-mouse (for FOXP3) secondary antibodies (Thermo Fisher Scientific) were used. Sections from corresponding tissue samples were also incubated with α-CD31 primary antibody (Santa Cruz Biotechnology Inc.) and stained with Alexa-488 α-goat secondary antibody (Thermo Fisher Scientific). Sections were visualised under 60X magnification in confocal microscope (Leica Microscope).

Cell viability assay

Sorted Treg cells were plated at a density of 1×10^4 cells/well of 96-well plates and incubated for different time intervals (12 h, 24 h, 36 h, 48 h, 60 h, 72 h). An MTT assay was performed to determine the viability of cells in culture at the said intervals. Effector T-cells were also kept as control for equivalent time points. MTT solution was added to each well (5 mg/ml) and the plates were incubated for 4 h at 37 °C. The MTT reaction was stopped and formazan crystals formed were dissolved with DMSO. The absorbance of each well was measured at 540 nm in Thermo Scientific Microplate reader using ScanIT Software. Percentage viability of Treg cells was obtained by comparing O.D. values with those from effector T-cells.

Statistical analyses

The values of data are shown as the standard error of the mean (SEM) except when otherwise indicated. The comparison of multiple experimental groups was performed by the I-way ANOVA test. This was followed by the Bonferroni post-hoc test. The Kaplan–Meier method was used to plot the survival probability graph for breast cancer patients that use gene expression data and relapse-free survival information from GEO, EGA, and TCGA [34]. Data were analyzed and, when appropriate, the significance of the differences between mean values was determined by a Student's *t* test. Results were considered significant at $p < 0.05$.

Results

Inter-relationship between Tregs and neo-angiogenesis in the breast tumor microenvironment

Various statistical facts clearly indicate that tumor-associated Treg cells play a significant role in tumor progression. A combination of phenotypic markers was used to define the Treg cells and their association with tumor progression. For this, we analyzed the expression of FOXP3, a master regulator of the suppressor properties of $CD4^+$ Treg cells, and the phenotypic markers IL2Rα (CD25). Post-operative breast tumor tissue samples were processed, and single cell suspensions obtained were used to detect presence of Treg cells by flow cytometry. Our immune-phenotyping studies showed an increased proportion of $CD4^+CD25^+FOXP3^+$ Treg cells in the tumor-site with advanced breast cancer (representative plots in Fig. 1a; respective controls for gating shown in Supplementary-1a).

Since tumor angiogenesis is a common phenomenon for most of the cancers, we next tried to understand the association between tumor-infiltrated Treg cells and neo-angiogenesis. Immunofluoresence study was performed on breast tumor tissue sections to study the levels of $CD4^+FOXP3^+$ cells and CD31 (endothelial cell marker). CD4 and FOXP3 were detected with different flourochrome-conjugated secondary antibodies in the same sections (Alexa 488 for CD4 and Alexa 594 for FOXP3) and CD31 was detected in another section of the same samples. It was observed that early stage breast tumor patients showed much lower presence of $CD4^+FOXP3^+$ cells, whereas Stage-IV (based on TNM classification) patients showed a much greater presence of these cells (representative images in Fig. 1b; upper and middle panels). Parallely CD31 expression also showed a similar pattern (representative image in Fig. 1b; lower panels). For a more quantitative representation we also calculated percentages of $CD4^+CD25^+FOXP3^+$ Treg cells and $CD31^+$ cells from a pool of 16 breast cancer patients. The data was segregated according to the stages of the patients and have been represented in Fig. 1c (left panel). Frequency of Treg cells and $CD31^+$ cells showed a highly positive correlation ($r = 0.8653$; $p < 0.0001$) (Fig. 1c; right panel).

The Kaplan–Mayer plot derived from GEO, EGA and TCGA database for breast cancer established a high-correlation of poor prognosis and poor patient relapse-free survival with the presence of high-abundance of CD31-positive endothelial cells (neo-angiogenesis) in the tumor microenvironment (Fig. 1d). In a parallel syngeneic mouse breast cancer model, it was observed that with the increase in tumor size angiogenesis also increased. The 4th-week tumor appeared to have more blood vessels than the 2nd- or 3rd-week tumors and also showed increased frequency of $CD31^+$ cells (Fig. 1e; left and middle panel). Percentages of $CD4^+CD25^+FOXP3^+$ and $CD31^+$ cells were calculated from flow cytometry data, and the correlation graph was plotted (Fig. 1e; middle and right panels). It was observed that there was a high correlation ($r = 0.9721$; $p < 0.0001$) between the frequency of Treg cells and CD31-positive endothelial cells in mouse breast tumor-site as well. Both human and mice system thus indicated a relationship between the augmentation of Treg cells and neo-angiogenesis with the advancement of the tumor. However, it is known that tumor cells themselves produce copius amounts of VEGFA. Expectedly, it was found that VEGFA secretion by 4T1 cells also co-related with $CD31^+$ cells (data shown in Supplementary-1b).

Tumor-associated Treg cells secrete pro-angiogenic factor VEGFA

The existence of inter-relationship between Treg cells and tumor-angiogenesis in both human and mouse breast cancers prompted us to investigate whether Treg cells have any role in instigating endothelial cells to undergo neo-angiogenesis. Since the production of VEGFA is the major driving factor for neo-angiogenesis, we wanted to identify whether there were any VEGFA-producing Treg cells present in the tumor microenvironment. To understand the nature of Treg cells in the tumor microenvironment, $CD3^+$ T-cells were sorted from breast tumor tissue of 10 breast cancer patients and flow cytometry was performed with additional phenotypic marker (CD127). We performed the t-distributed Stochastic Neighbour End-Joining (tSNE) analysis, which combines the multi-colour flow-cytometric data from the different samples and displays it as a 2-D plot representing the distribution of different marker expressions. As shown in Fig. 2a, the tSNE plot for $CD4^+$ cells was displayed as a contour plot. Based on unsupervised clustering of various sub-populations according to marker expression, we detected that apart from a cluster of $CD4^+CD25^+CD127^-FOXP3^+$ Treg (shown in cyan) cells,

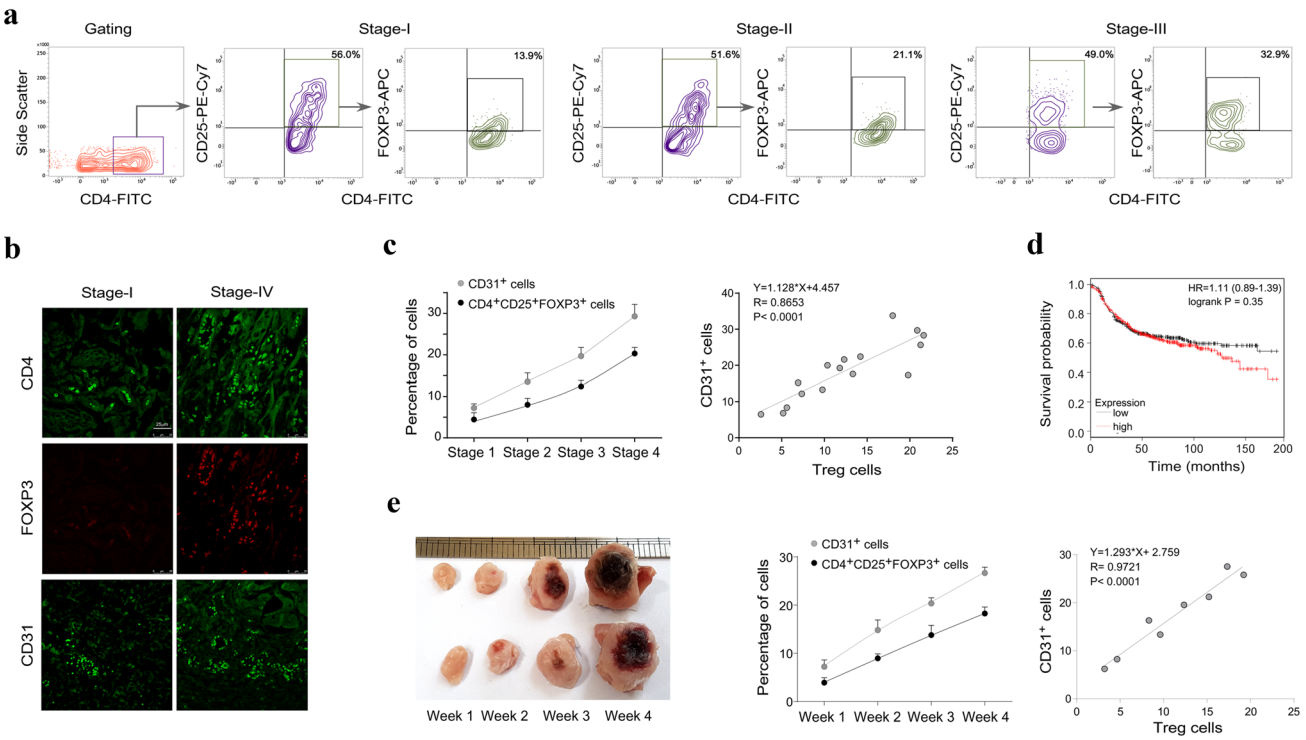

Fig. 1 Inter-relationship between Treg and neo-angiogenesis in the breast cancer microenvironment. **a** Representative flow-cytometric data are showing gating strategy and percentages of $CD4^+CD25^+FOXP3^+$ Treg cells among infiltrating lymphocytes from different stages of human breast cancers. Numbers indicate the percentage of cells among the $CD4^+$ population. **b** Representative immunoflouresence images of Stage-1 and Stage-4 breast tumor tissue samples show expression of CD4 (upper panel) and FOXP3 (middle panel) in the same tissue sections and CD31 expression (lower panel) in other sections from corresponding samples. **c** Mean percentages of $CD4^+CD25^+FOXP3^+$ cells and $CD31^+$ cells obtained from flow cytometry data of different stage tumor tissue samples (left panel) and correlation between the two (right panel; $n=16$). **d** Kaplan–Meier plot shows a high-correlation of poor prognosis and poor patient relapse-free survival with the presence of high-abundance of CD31-positive endothelial cells in the tumor microenvironment. **e** 4T1 tumor volume increase as mice breast cancer progresses (left). Percentages of $CD4^+CD25^+Foxp3^+$ cells and $CD31^+$ cells obtained from flow cytometry data of corresponding tissue samples (middle) and the correlation between them (right; $n=8$). Values are mean ± SEM of three independent experiments in each case or representative of a typical experiment

there was another cluster of cells (shown in red) which showed VEGFA expression in addition to the regular Treg markers. This indicated the presence of a separate population of VEGFA-producing Treg cells within the tumor micro-environment. When data from individual samples were considered, it was seen that there was a successive increase in the $CD4^+CD25^+CD127^-FOXP3^+VEGFA^+$ cell fraction in the advanced stages of tumor. The presence of $VEGFA^+$ Treg cells co-related with successive stages of the tumor, i.e., they were present in much higher frequency in Stage-II and Stage-III tumor tissues compared to Stage-I (Fig. 2b; representative FACS plots in Fig. 2c; respective controls in Supplementary-1c). To determine the level of secreted VEGFA, serum was isolated from the peripheral circulation of various stages of breast tumour patient, and the level of VEGFA was analysed by ELISA. It was observed that with the progression of breast cancer, secretion of pro-angiogenic VEGFA increased significantly (Fig. 2d).

Quantification of VEGFA production by Treg cells

Treg cells and effector-T cells were sorted from peripheral blood of breast cancer patients and age/sex-matched healthy-individuals, respectively, and cultured ex-vivo. (Viability percentages of Treg cells in ex-vivo culture shown in Table 1). The amount of VEGFA produced in the culture media was measured by ELISA (Fig. 3a). The results showed that purified Treg cells from breast cancer patients, secrete high-amount of VEGFA in comparison to effector T-cells or Tregs from healthy individuals, cultured in similar condition. The expression of VEGFA in effector T-cells and Treg cells was further ascertained by confocal microscopy. Purified cells were treated with BrA/PMA/ionomycin to block the extracellular secretion of the VEGFA produced by the cells. It was observed that Treg cells from patient blood express a significantly higher amount of VEGFA than that of their normal counterparts (Fig. 3b). Purified naive T-cells, obtained from peripheral blood of healthy individuals were

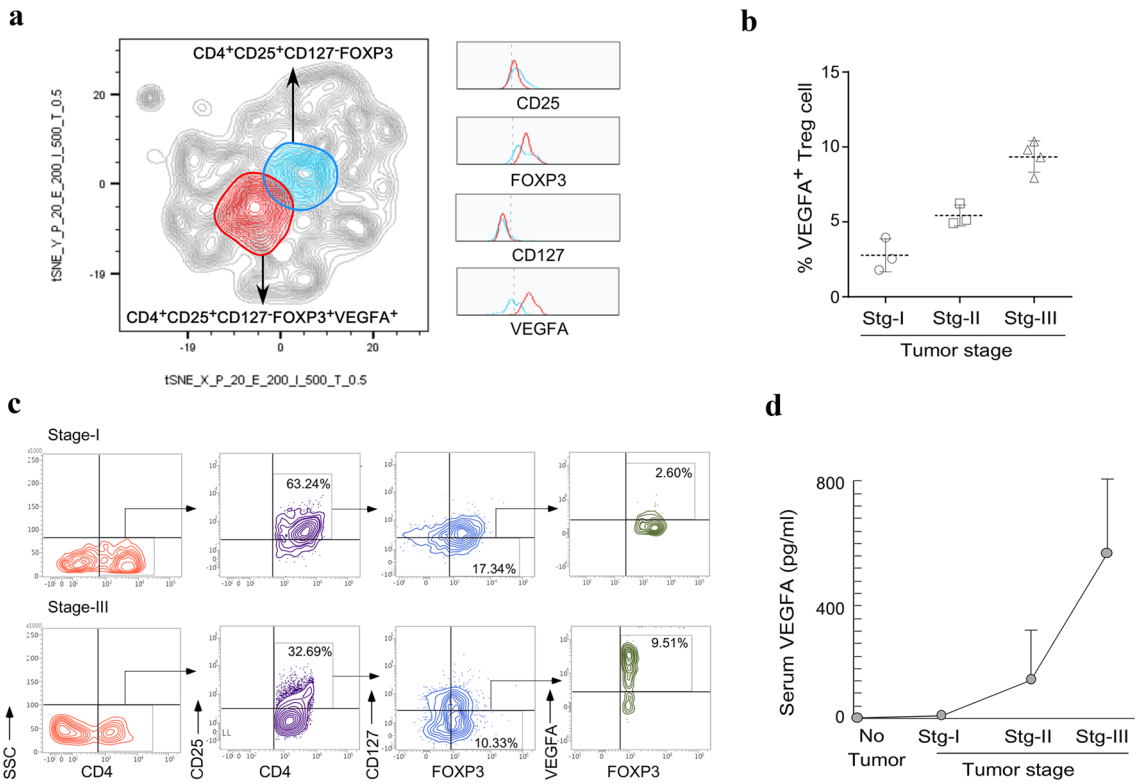

Fig. 2 Breast tumor-associated Treg cells secrete pro-angiogenic factor VEGFA. **a** tSNE plot showing the distribution of various marker expression in $CD4^+$ T-cells from breast tumor patients. The tSNE plot for $CD4^+$ cells was displayed as a contour plot (grey lines). Based on the distribution of these populations, two query gates were drawn. The population marked in cyan signified the conventional $CD4^+CD25^+CD127^-FOXP3^+$ population and population marked in red signifies $CD4^+CD25^+CD127^-FOXP3^+VEGFA^+$ population. Histogram plots show difference in marker expression of the two populations. **b** Graphical representation of $CD4^+CD25^+CD127^-FOXP3^+VEGFA^+$ Treg cells in different stages of breast tumor ($n=10$). **c** Representative flow-cytometric representation of $CD4^+CD25^+CD127^-FOXP3^+VEGFA^+$ Treg cells in breast cancer patients of stage-1 and stage-3 tumor. **d** ELISA performed from serum samples of breast tumor patients shows expression of pro-angiogenic factor VEGFA in different grades of tumor. Values are mean ± SEM of three independent experiments in each case or representative of a typical experiment

Table 1 Percentage viability of Treg cells in ex-vivo culture

Time (h)	12	24	36	48
Viability of Treg cells (%)	99.24	88.51	86.23	81.69

Values are the mean of three independent experiments in each case

activated by anti-CD3 and anti-CD28 stimulation and cultured with cell-free supernatants from cultured breast tumor cells (conditioned media) and kept for different time intervals to detect populations of VEGFA producing Treg cells. Flow-cytometry data showed a steady increase of $CD4^+CD25^+FOXP3^+VEGFA^+$ population of cells with time (Fig. 3c). All these data indicate that Treg cells are capable of producing the pro-angiogenic factor VEGFA. A parallel experiment with the cells kept under similar conditions but without the tumor conditioned media showed slight expression of FOXP3, but no significant expression of VEGFA by the $FOXP3^+$ cells (data shown in Supplementary-1e).

The mechanism behind the secretion of VEGFA from Treg cells in the tumor microenvironment

It is evident from our previous results that Treg cells secrete high-level of VEGFA, but the mechanism by which VEGFA-mRNA is transcribed in these cells remains elusive. FOXP3 is the key transcriptional regulator of Treg cells and is responsible for inducing the expression of several Treg-associated suppressive factors. Since our previous results showed that FOXP3-expressing Treg cells produced VEGFA, we wished to identify whether FOXP3 has any specific role in regulating VEGFA transcription in these Treg cells or not. To validate our assumption, FOXP3 was ablated in Treg cells by shRNA, and the expression of VEGFA was visualized by confocal microscopy. It was observed that the level of VEGFA decreased in FOXP3 ablated Treg cells (Fig. 4a). Thus it was clear that the presence of FOXP3 is essential for VEGFA expression in Treg cells. To

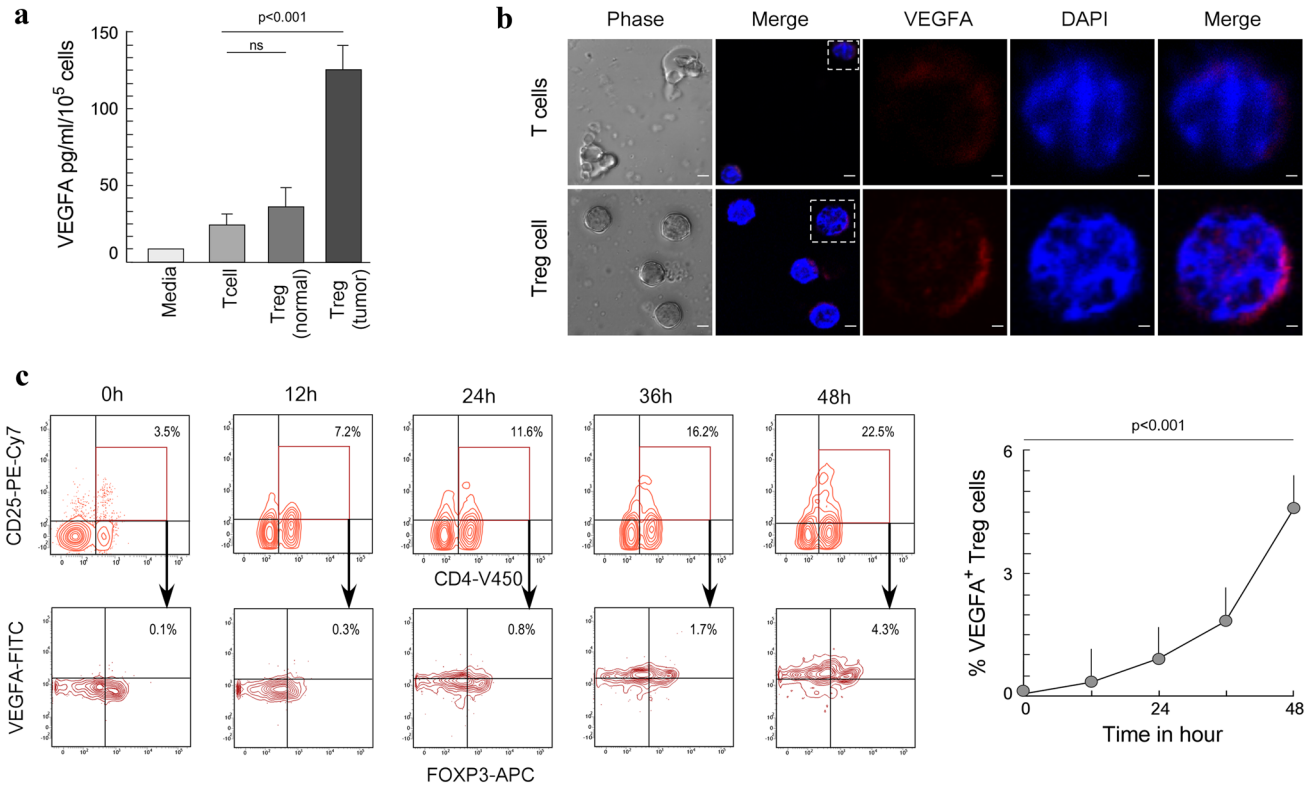

Fig. 3 Quantification of VEGFA production by Treg cells. **a** levels of VEGFA secreted in cell culture media post 72 h culture of effector T-cells obtained from healthy volunteers and Treg cells obtained from peripheral blood of healthy volunteers (normal) and breast cancer patients (tumor), respectively. **b** Confocal images of effector T-cells and Treg cells stained with Alexa-546-conjugated anti-VEGFA antibody. Image magnification: × 60; scale bar 10 µm. **c** Developmental profile of VEGFA$^+$ Treg cells generated from naïve T-cells obtained from peripheral blood of healthy individuals (activated with anti-CD3 and anti-CD28) and kept in ex-vivo culture with cell-free supernatants (conditioned media) from cultured breast cancer cell lines (left), graphical representation of the developmental profile of VEGFA$^+$ Treg cells (right). Values are mean ± SEM of three independent experiments in each case or representative of a typical experiment

understand the transcriptional regulation, the VEGFA promoter was analyzed using rVISTA and MatInspector, a Cold Spring Harbor Laboratory promoter database. The result showed that the VEGFA promoter does not have any FOXP3-binding site. However, there was a putative STAT3-binding site at the VEGFA promoter (Fig. 4b). Though the promoter analysis data suggested that FOXP3 could not directly bind to VEGFA promoter, experimental data suggested that FOXP3 was essential for VEGFA expression, creating a paradox. Hence, to have further insight regarding VEGFA regulation in Treg cell, FOXP3 interacting protein partners were deduced using STRING 11.0, Innate DB, and Bio-GRID 3.2 database. Interactions between transcription factors in different T cell subsets were obtained from STRING 9.1 and modeled using Cytoscape v3.1.0 software. We can clearly observe that STAT3 is one of the interacting partners of FOXP3 (Fig. 4c). We hypothesized that FOXP3 might be interacting with STAT3 to occupy VEFGA promoter to activate its transcription. To test this hypothesis, purified Treg cells from peripheral blood of breast cancer patients were transfected with shRNA clones against FOXP3/STAT3 and cultured in the presence of breast tumor cell-free supernatants. Relative expression of VEGFA transcript was significantly decreased in both the FOXP3 and STAT3 ablated Treg cells (Fig. 4d). To unfurl the transcriptional regulation of VEGFA in Treg cells, the following experiments were performed. To confirm the interaction between FOXP3 and STAT3 confocal microscopy and co-immunoprecipitation studies were performed. The confocal microscopy data showed the increased nuclear co-localization of FOXP3 and STAT3 in Treg cells, while in the T-cell population, such association of FOXP3 and STAT3 was less (Fig. 4e). The co-immunoprecipitation and Western blot study confirmed a significant association between STAT3 and FOXP3 in Treg cells (Fig. 4f). This confirmed the interaction between FOXP3 and STAT3. Next, to determine the direct involvement of these two partners in VEGFA transcription, we performed the ChIP-reChIP analysis. The results in Fig. 4g showed that FOXP3 formed a complex with STAT3 that was recruited to the VEGFA promoter in Treg

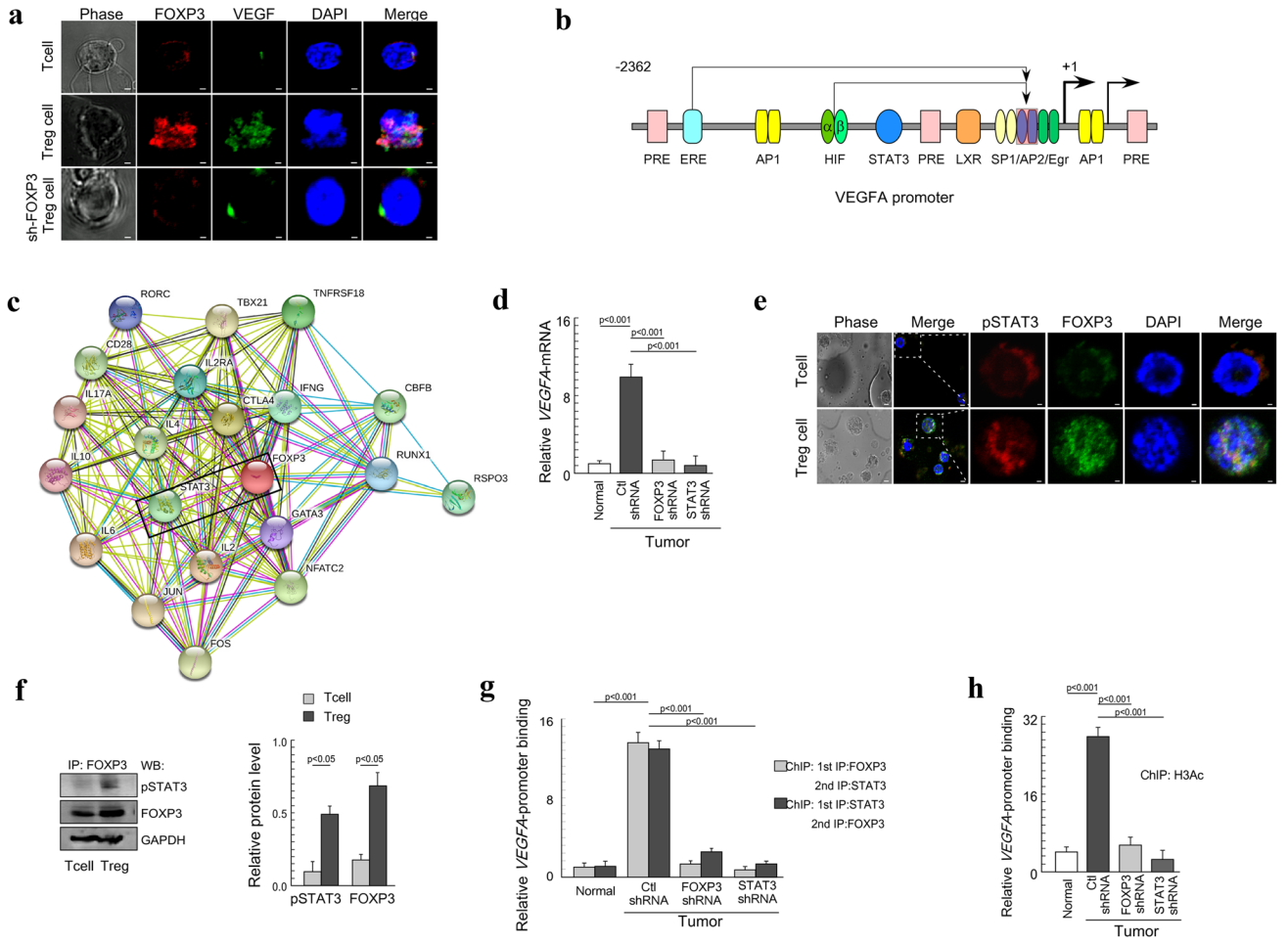

Fig. 4 FOXP3 in association with STAT3 induces *VEGFA* transcription in the tumor microenvironment. **a** Confocal images represent the expression level of intracellular FOXP3 (Alexa-546), and VEGFA (Alexa-488) in T-cell, Treg cell, and FOXP3 ablated Treg cells. Image magnification: × 60; scale bar 10 µm. **b** VEGFA promoter binding-site obtained using RVISTA and Mat inspector algorithm. VEGFA promoter has response elements and transactivating factors. Response elements are PRE (progesterone response element; TGTACA, TGTACA, TGTTCT; − 1865/− 1860, − 716/− 711, + 679/ + 684), ERE (estrogen response element; AAT CAGACTGAC; − 1525/− 1514), Egr (Early growth response; CCG GGGGC; − 77/− 70). Transactivating factors are: AP-1 (activator protein 1; TGAATCA, TGAGTGA; − 1168/− 1015, + 418/ + 425), HIF (hypoxia inducible factor; TACGTGGG; − 975/− 968), STAT3 (signal transducer and activator of transcription-3; TTCCCA AA; − 848/− 840), LXR (liver × receptors; TGTCCGcacgTAA CCT; − 317/− 302), Sp1 (specificity protein-1; GGGGGCCGCCC; − 238/− 233, 94/− 89, − 84/− 79, − 73/− 68, − 57/− 52), AP-2 (activator protein-2; GGCCGGGG; − 79/− 72). **c** FOXP3 interacting protein partners were deduced using STRING 11.0, Innate DB, and Bio-GRID 3.2 database. **d** The expression level of *VEGFA*-mRNA in T-cells, Treg cells, FOXP3-/STAT3-ablated Treg cells were determined by qPCR. **e** Confocal images show the expression of FOXP3 (Alexa-488) and pSTAT3 (Alexa-546) in T-cells and Treg cells. Image magnification: × 60; scale bar 10 µm. **f** Western blot result shows an association between FOXP3 and pSTAT3 in T-cells and Treg cells. Densitometry analysis of FOXP3/pSTAT3 normalized to GAPDH. **g** Chip/re-Chip experiment was performed to evaluate STAT3-FOXP3 interaction at STAT-binding site of *VEGFA* promoter. **h** ChIP assay was performed to study histone modification at *VEGFA* promoter. T-cells and Treg cells for these assays were isolated from peripheral blood of healthy individuals and breast cancer patients, respectively. Tregs were cultured in the presence of cell-free supernatants (conditioned media) from cultured breast cancer cell lines. Values are mean ± SEM of three independent experiments in each case or representative of a typical experiment

cells. Histone-3 was also hyperacetylated at the STAT3-binding site on VEGFA promoter, and such acetylation was found to be perturbed in the FOXP3, and STAT3 ablated conditions which indicated that the FOXP3-STAT3 co-association plays an important role in chromatin modification and activation of VEGFA promoter in Treg cells (Fig. 4h).

VEGFA secreted from Treg cells promotes neo-angiogenesis

Previous results indicate that Treg cells produced abundant VEGFA in the tumor microenvironment. Next, we aimed to determine the involvement of this Treg-secreted VEGFA in the induction of neo-angiogenesis. To elucidate the role

of Treg cell-secreted VEGFA in neo-angiogenesis, sprout formation, endothelial cell migration, and ex-vivo CAM assays were performed. These are considered as prime assays to study neo-angiogenesis. Endothelial cells respond to VEGFA secreted by itself or surrounding cells by forming sprouts. Sprouts comprise of tip, stalk, and phalanx cells. In our experiment, to mimic cellular conditions, endothelial cells were embedded in matrigel. To this end, matrigel embedded endothelial cells were treated with VEGFA (10 ng/ml) and Treg cells, T-cells, or VEGFA-neutralized Treg cells supernatant and were observed for sprout formation (Fig. 5a; upper panels). To perform wound healing assay, endothelial cells were grown to confluence in 12 well plates. Then they were serum starved for 24 h and wounded using micro-tip. Cells were washed and replenished with fresh serum-free media with recombinant VEGFA, T-cell, Treg cell, VEGFA-neutralized Treg cells supernatant. Images were taken after 18 h (Fig. 5a; lower panels). Results showed that both the sprout formation and cell migration were significantly increased by Treg spent medium. However, VEGFA-neutralization in Treg spent medium specifically blocked such enhanced sprout formation and cell migration, which validated the involvement of Treg-secreted VEGFA in the induction of sprout formation and endothelial cell migration. The number of sprouts formed and endothelial cell migrated were counted and plotted graphically (Fig. 5a; right panels). For further confirmation of the role of Treg-secreted VEGFA-mediated new blood vessel formation, we performed a chick chorioallantoic membrane (CAM) assay. It was observed that treatment of Treg supernatant leads to the intrusion of a new blood vessel in chick embryo (Fig. 5b; left). Quantification of number and length of tubule complex by Angioquant software (http://www.cs.tut.fi/sgn/csb/angioquant/; 26) also showed a coherent pattern with the neo-angiogenesis (Fig. 5b; right).

Targeting Treg cells reduces tumor growth and alters angiogenesis pattern in tumor tissue

To understand the role of Tregs in promoting tumor angiogenesis, we utilized Foxp3-shRNA which were packaged into lentiviral clones and delivered intravenously to 4T1 tumor-bearing BALB/C mice. By targeting Foxp3 in circulating PBMC, we tried to achieve the depletion of Treg cells. Parallely, a Foxp3 ectopic over-expression clone was also delivered in another set of mice to observe the effect of increasing Treg cells. As shown in Fig. 6a, mice receiving Foxp3-shRNA showed stunted growth of tumor, whereas those receiving FoxP3 over-expression clones had an enhanced tumor growth compared to control sets. Moreover, flow cytometry data showed that Foxp3-shRNA successfully reduced percentages of Treg cells within the tumor tissue infiltrating lymphocytes, while Foxp3-cDNA had the opposite effect (representative FACS plots

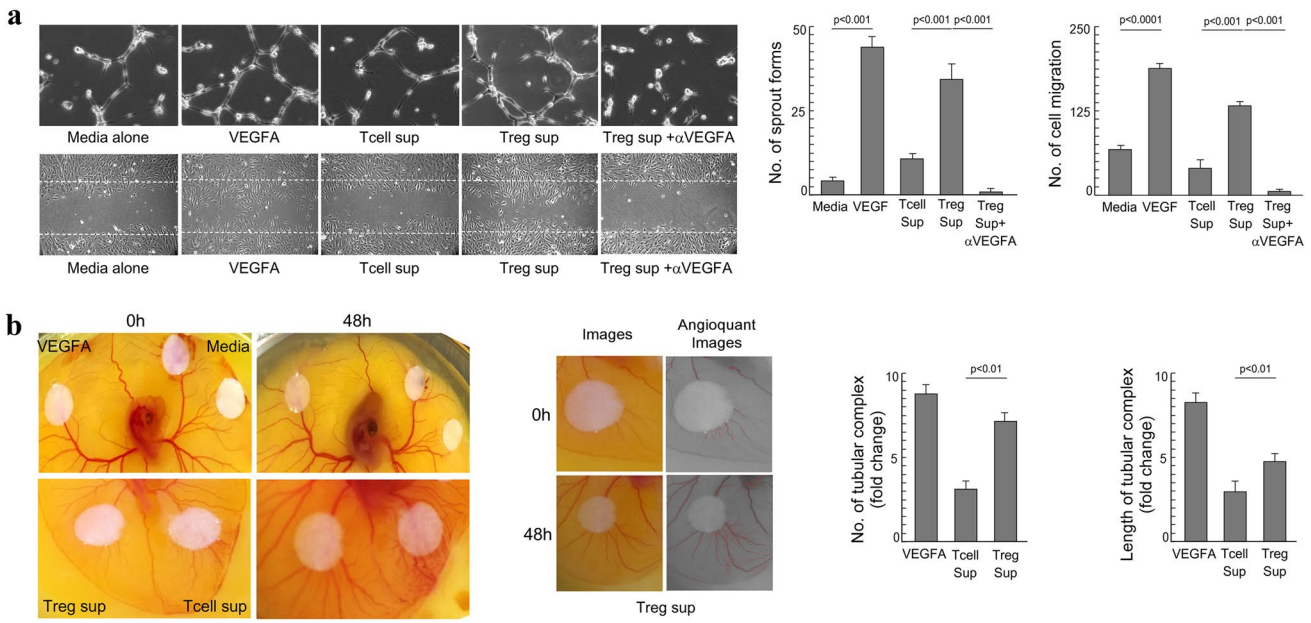

Fig. 5 VEGFA secreted from Treg cells promotes neo-angiogenesis. **a** Sprout formation (upper panels) and wound healing assay (lower panels) was performed in the presence of VEGFA (10 ng/ml), T-cell and Treg cell spent-media, and VEGFA-neutralized Treg spent media with human umbilical vein endothelial cells. The number of sprouts formed (middle) and endothelial cell migrated (right) were calculated and plotted graphically. **b** CAM assay was performed to study ex-vivo new blood vessel formation. Number and length of tubule complexes were quantified using the Angioquant software. Values are mean ± SEM of three independent experiments in each case or representative of a typical experiment

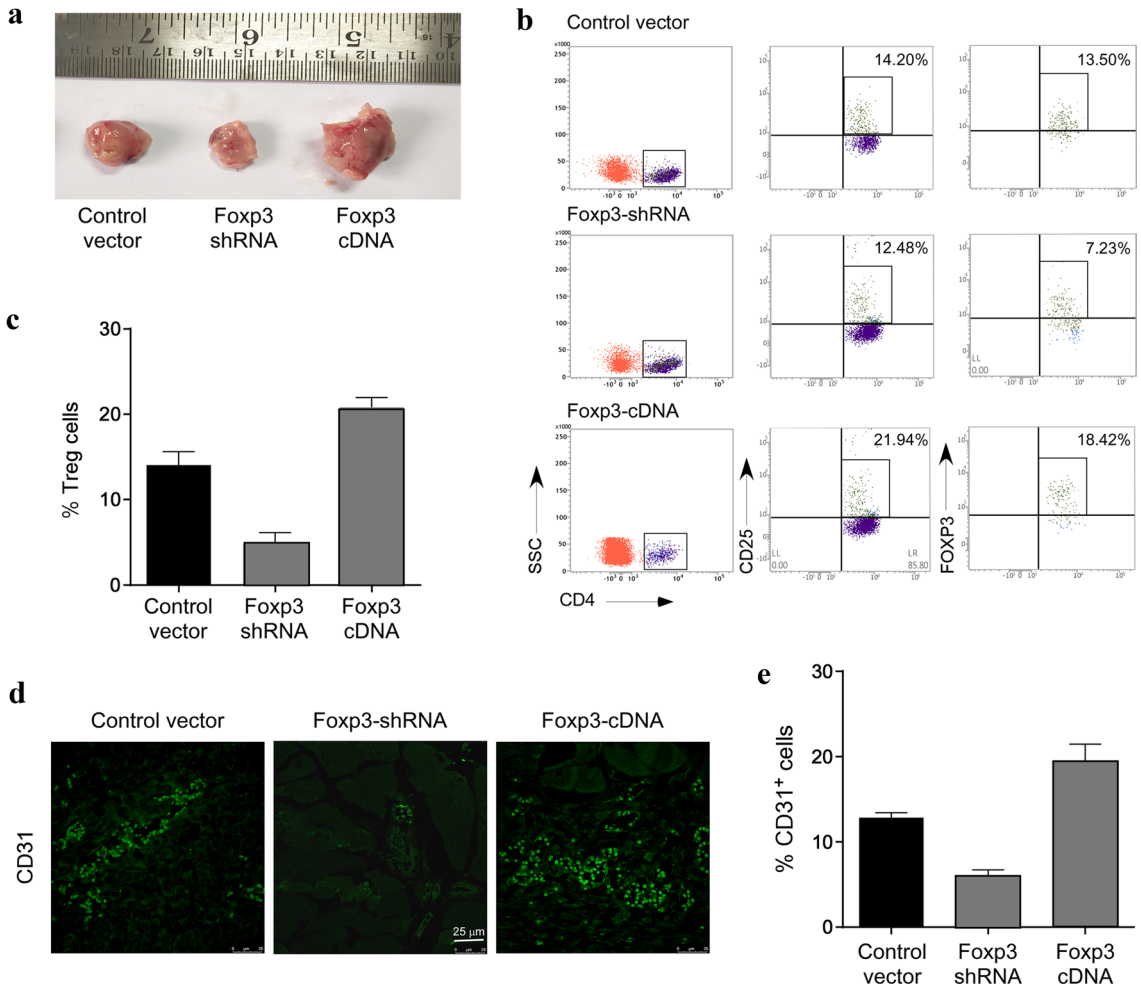

Fig. 6 Treg depletion in the mouse tumor model shows reduced tumor angiogenesis. **a** Representative images of tumor size after 4 weeks in 4T1 tumor-bearing mice receiving Foxp3 shRNA/Foxp3 cDNA/control lentiviral clones. **b** Representative flow cytometry plots showing percentages of $CD4^+CD25^+FOXP3^+$ Treg cells at the tumor site of 4T1 tumor-bearing mice receiving Foxp3 shRNA/Foxp3 cDNA/control lentiviral clones. **c** Graphical representation of percentages of $CD4^+CD25^+FOXP3^+$ Treg cells at the tumor site of 4T1 tumor-bearing mice receiving Foxp3 shRNA/Foxp3 cDNA/control lentiviral clones ($n=3$). **d** Representative images of immunofluorescence staining showing expression of CD31 in tumor tissue sections from 4T1 tumor-bearing mice receiving Foxp3 shRNA/Foxp3 cDNA/control lentiviral clones. **e** Graphical representation of percentages of $CD31^+$ cells (obtained from flow cytometry data) of 4T1 tumor-bearing mice receiving Foxp3 shRNA/Foxp3 cDNA/control lentiviral clones ($n=3$)

in Fig. 6b and Treg cell percentages in Fig. 6c). Interestingly, it was observed that mice with lower Treg percentages (receiving Foxp3-shRNA) also showed significantly low expression of the angiogenesis marker CD31, whereas Foxp3 over-expressing mice showed much higher CD31 expression, as evident from immunofluoresence images of tumor tissue sections (Fig. 6d). Percentages of $CD31^+$ cells obtained from flow cytometry of single cell suspensions from mouse tumor tissue also showed a similar pattern (Fig. 6e). This clearly indicated that the presence/absence of Tregs not only influenced tumor growth but also had an effect on the angiogenesis pattern in the tumor tissue.

Discussion

Tumor and stromal cells (fibroblasts, myofibroblasts, epithelial, endothelial, immune cells, and extra-cellular matrix) play an important role in tumor progression. These cells are normal until and unless they undergo "angiogenic-switch" [21, 35]. Abnormal growth of cancer cells causes increased interstitial fluid pressure on vessels which breaches the blood vessels. It results in central hypoxia, which facilitates secretion of pro-angiogenic factor VEGFA; thus triggers "angiogenic switch". Furthermore, transcription of silent genes takes place, and

the expression of normal genes get altered. As a result, secretion of the plethora of chemokines, immunosuppressive cytokines and angiogenic factors (i.e., CCL22, IL10, TGFβ, IL35, and VEGFA) promotes infiltration of immune cells like macrophages, dendritic cells, natural killer (NK) cells, myeloid-derived suppressor cells and Treg cells in tumor microenvironment to promote tumor growth [20].

In the tumor microenvironment, the presence of Treg cells inhibits an immunogenic response to the tumor, which translates into the poor prognosis of cancer. Several studies have shown that the presence of Treg cells is associated with a more aggressive and metastatic form of cancer and leads to poor patient survival. In breast cancer patients, $FOXP3^+$ Treg cells are an important prognostic marker in both invasive and non-invasive cancer [13]. A higher number of tumor-Treg cell relates to poor survival of ovarian cancer patients [14]. In prostrate, ovarian and gastric cancer patients Treg cells infiltrate the tumor through CCL22-CCR4 axis. In gastric cancer patients as well, Treg cells are associated with vascular/lymphatic/perineural (VELIPI) invasion and lower disease-free survival [18]. A similar profile of Treg cells is observed in renal [36, 37], hepatocellular [38], and other types of cancer. Overall, the presence of Treg cells is an indication of tumor metastasis and relapse. In addition to the secretion of various immunosuppressive factors, tumor-associated Treg secretes pro-angiogenic factor VEGFA, which instigates endothelial cells from the existing blood vessel to develop new branches of blood vessels to form neo-angiogenesis.

Prevalence of Treg cells in almost every type of cancer and its connection with the development and aggressiveness of cancer prompted us to investigate its role in neo-angiogenesis and the mechanism behind the expression of pro-angiogenic factor VEGFA. Treg cells are characterized by the expression of CD4/CD25/FOXP3. They secrete cytokine TGFβ, IL10, IL35 [39, 40] which are indispensable for its acquired immunosuppressive properties. These specialized cells also secrete VEGFA, a pro-angiogenic factor required for the development of tumor-angiogenesis. In the present study, we characterized the marker profiles of Treg cells isolated from the breast tumor microenvironment. It was observed that the population of Treg cells increases with the advancement of cancer. We also noticed a positive co-relation between the presence of Tregs and angiogenesis. As the size of the tumor increases, it requires neo-angiogenesis for the supply of oxygen and nutrients. The tumor also exploits peripheral circulatory-route for metastasis to become malignant. Interestingly, Kaplan–Meier plot derived from GEO, EGA, and TCGA database for breast cancer showed a high-correlation of poor relapse-free survival with the presence of high-abundance of neo-angiogenesis in tumor-site. Hence we were interested in probing whether the Treg cells present in tumor micro-environment contributed to the pool of VEGFA that caused neo-angiogenesis.

The t-distributed Stochastic Neighbour End-joining (tSNE) analysis is a powerful machine learning algorithm for dimensionality reduction that is suitable for visualizing multi-dimensional flow-cytometry data containing several parameters in a 2-dimensional plot while maintaining the structure of the data [26, 41]. Using this technique, we analyzed our multi-color flow-cytometry data, which is represented as a distribution on a 2-D plot and particular areas in the plot represent distinct cell populations showing a different combination of marker signature. Since human effector T cells are sometimes known to transiently express FOXP3, we incorporated CD127 as an additional marker to exclude such populations. It was observed that in addition to the conventional Treg cell population expressing the widely accepted markers $CD4^+CD25^+CD127^-FOXP3^+$, there was also a population of Treg cells that was showing additional expression of VEGFA. It is thus highly probable that conventional Treg cells acquire the capability to express VEGFA in the tumor micro-environment, and such VEGFA-secreting Treg population might be a contributing factor that promotes angiogenesis at the tumor-site. From the laboratory, it was previously reported that FOXP3 in association with STAT3 induces transcription of IL10 in Treg cells [17]. Similar to IL10, VEGFA promoter region also lacks FOXP3-binding site and has STAT3-binding site. Instead of direct promoter-occupancy, we found that FOXP3 promotes VEGFA transcription by associating with a locus-specific transcription factor STAT3, in Treg cells from breast cancer patients. Our data thus suggests that the FOXP3-STAT3 alliance serves as an important transcriptional regulator that enhances the production of VEGFA.

In this study, we focused on the interrelationship between Treg cells and endothelial cells. Sprout formation, migration of endothelial cells, and CAM assays are primary in-vitro and ex-vivo assays to study the neo-angiogenesis. VEGFA secreted from Treg cell leads to endothelial cell sprout formation and migration and ultimately lead to new blood vessel formation. The present study thus provides an insight into the interaction between the immunosuppressive Treg cells and endothelial cells and sheds new light on a special sub-population of VEGFA secreting Treg present in breast tumor patients. The study also establishes the mechanism by which the FOXP3-STAT3 complex is responsible for the induction of VEGFA transcription by Treg cells.

Moreover, to probe the actual contribution of Treg cells to tumor angiogenesis, we also tried to deplete Foxp3-expressing Treg cells in tumor bearing mice through lentiviral shRNA clones. Lentiviral particles encoding shRNAs targeted against Foxp3, when delivered through tail-vein could effectively reduce levels of Tregs in mice. Correspondingly we found that mice with depleted Tregs showed a lower

volume of tumor as well as lower percentages of angiogenesis markers. A reverse effect was seen in case of mice receiving Foxp3 over-expression clones. This experiment suggested that Tregs definitely have an inter-relationship with tumor angiogenesis. Although several other immune cells, as well as tumor cells themselves are capable of producing VEGFA, we can thus consider that presence of high levels of Tregs sufficiently adds to the pool of VEGFA and increases the rate of tumor-angiogenesis. We acknowledge that the effect of depleting Tregs may be indirect also by relieving immunosuppression and boosting other host immune cells to restrict tumor growth thereby lowering neo-angiogenesis.

A study by Li et al. [42] claims that FOXP3 inhibits angiogenesis by downregulating VEGF in breast cancer. While this may seem contradictory to our findings, a closer look reveals that the authors have shown that FOXP3 can inhibit VEGF production by tumor cells only, while we report production of VEGFA by Treg cells present in the tumor micro-environment. Thus, even if FOXP3-expressing breast tumor cells produce lower VEGFA, the presence of VEGFA-secreting Treg cells in the tumor micro-environment can significantly add toVEGFA pool. In our unpublished data we observed that a portion of breast cancer cells which showed stem cell-like phenotype express FOXP3, and these cells are restricted to proliferation. Moreover, regulation of a gene by transcription factors is highly dependent on the context and epigenetic status of the cell. Thus the mechanism regulation of VEGFA by FOXP3 in tumor cells might be completely different from what we have shown in Treg cells.

Conclusions

Tumor cells have the potential for uncontrolled cell proliferation. They can migrate or metastasize to vital organs, which leads to poor prognosis of the disease. Neo-angiogenesis provides an adequate amount of oxygen and nutrients which acts as a major determinant for proliferation, migration, and metastatis of cancer cells. An increase in tumor size causes hypoxic stress in tumor cells, and this leads to the secretion of chemokines, which attract T-regulatory (Treg) cells in the tumor-site. Treg cells implement immunosuppressive and tumor-promoting strategies. Apart from several immunosuppressive properties of Tregs, our study indicates that Tregs from breast tumor patient tissue and blood produces significant amount of VEGFA. We also elucidate the transcriptional mechanism of *VEGFA* expression in Treg cells. The lineage-specific transcription factor FOXP3 in association with locus-specific transcription factor STAT3 binds to *VEGFA* promoter to induce its transcription. Treg secretes pro-angiogenic factor VEGFA that promotes neo-angiogenesis under in-vitro conditions and modulating Treg levels in tumor-bearing mice reduced tumor growth as well as angiogenesis at tumor site.

Acknowledgements The authors are grateful to K. Jana for providing access to mice facility in Bose Institute. Authors are also thankful to A.K. Poddar for providing technical support in confocal imaging and R.K. Dutta for providing technical support in flow-cytometry.

Author contributions KK: formulated the project, designed and performed the experiments, analyzed data and wrote the manuscript; SB: performed flow-cytometry and qPCR related experiments, analysed data, provided support in CAM experiments and edited the manuscript; AKP: provided support in in vivo experiments, immunology related techniques and gave critical suggestions; DC: performed co-immunoprecipitation and immunohistochemistry experiments; SC: performed chromatin immunoprecipitation experiments; SP: performed immunofluoresence experiments on tissue sections; TS and SD: prepared lentiviral/retroviral particles and helped in Treg depletion experiments; DR: collected and handled patient tissue and blood samples and helped in flow cytometry experiments; SS: provided support in handling human breast tissue samples and gave critical suggestions; GS: conceptualized the project, designed the experiments, analysed data and edited the manuscript.

Funding This work was supported by a research Grant from the Department of Biotechnology, Government of India.

Compliance with ethical standards

Conflict of interest The authors declare that they have no conflict of interest.

Ethical approval Ethical approval for collection of post-operative breast tumor tissue samples and peripheral blood from breast cancer patients/healthy female volunteers and subsequent experiments with them for this study was sanctioned under the provision of ethics committee, ESI Post Graduate Institute of Medical Science and Research, Kolkata, India (Approval No: ESI-PGIMSR/MKT/IEC/13/2017 dated: 22 Dec, 2017) and Human Ethics Committee, Bose Institute (Approval No: BIHEC/2017-18/5, dated: 28 May, 2017). Collection of samples from patients with localized disease and from healthy female volunteers and subsequent experimental procedures were in compliance with the Helsinki Declaration (http://www.wma.net/en/30publications/10policies/b3/).

Ethical standards
All animal (BALB/c mice) experiments were performed following Principles of laboratory animal care (NIH publication no. 85–23, revised in 1985) as well as Indian laws on 'Protection of Animals' under the provision of the Bose Institute Ethics Committee for the purpose of control and supervision of experiments on animals (Reg. no. 95/99/CPCSEA; Approval no: IAEC/BI/24/2015, dated: 26 May, 2015).

Informed consent Written Informed consent (IRB-1382) was obtained prior to sample collection from all individual participants included in the study. As per provisions of the consent forms, the participants agreed to donate peripheral blood/tissue samples for research purposes and did not restrict the authorized use of any data or results that arise from this study on condition of confidentiality of identity and personal health records. The personal identity of participants has not been disclosed anywhere in this study.

Animal source BALB/c mice, weighing 20–25 g, were obtained from the Central Translational Animal Research facility of Bose Institute, India.

Cell line authentication Human umbilical vein endothelial cells (HUVECs) were purchased from (Proforma Inv. no: 000075), HiMedia, India. The cells were authenticated by their cobblestone-like structure and Von Willebrand Factor, and CD31 positivity. Mouse mammary epithelial cancer cell 4T1 were obtained from ATCC. MCF-7 cells were obtained from National Center for Cell Science (NCCS), Pune, India.

References

1. Zhu J, Paul WE (2008) CD4 T cells: fates, functions, and faults. Blood 112:1557–1569. https://doi.org/10.1182/blood-2008-05-078154
2. Ondondo B, Jones E, Godkin A, Gallimore A (2013) Home sweet home: the tumor microenvironment as a haven for regulatory T cells. Front Immunol 4:197. https://doi.org/10.3389/fimmu.2013.00197
3. Sakaguchi S, Sakaguchi N, Asano M, Itoh M, Toda M (1995) Immunologic self-tolerance maintained by activated T cells expressing IL-2 receptor alpha-chains (CD25). Breakdown of a single mechanism of self-tolerance causes various autoimmune diseases. J Immunol 155:1151–1164
4. Zheng Y, Rudensky AY (2007) Foxp3 in control of the regulatory T cell lineage. Nat Immunol 8:457–462
5. Sakaguchi S, Miyara M, Costantino CM, Hafler DA (2010) FOXP3+ regulatory T cells in the human immune system. Nat Rev Immunol 10:490–500. https://doi.org/10.1038/nri2785
6. De Palma M, Biziato D, Petrova TV (2017) Microenvironmental regulation of tumour angiogenesis. Nat Rev Cancer 17:457–474. https://doi.org/10.1038/nrc.2017.51
7. Wang M, Zhao J, Zhang L, Wei F, Lian Y, Wu Y, Gong Z et al (2017) Role of tumor microenvironment in tumorigenesis. J Cancer 8:761–773. https://doi.org/10.7150/jca.17648
8. Hillen F, Griffioen AW (2007) Tumour vascularization: sprouting angiogenesis and beyond. Cancer Metastasis Rev 26:489–502
9. Bielenberg DR, Zetter BR (2015) The contribution of angiogenesis to the process of metastasis. Cancer J 21:267–273
10. Zetter BR (2008) The scientific contributions of M. Judah Folkman to cancer research. Nat Rev Cancer 8:647–654. https://doi.org/10.1038/nrc2458
11. Petrova V, Annicchiarico-Petruzzelli M, Melino G, Amelio I (2018) The hypoxic tumour microenvironment. Oncogenesis 7:10. https://doi.org/10.1038/s41389-017-0011-9
12. Facciabene A, Peng X, Hagemann IS, Balint K, Barchetti A, Wang LP et al (2011) Tumour hypoxia promotes tolerance and angiogenesis via CCL28 and T(reg) cells. Nature 475:226–230
13. Bates GJ, Fox SB, Han C, Leek RD, Garcia JF, Harris AL, Banham AH (2006) Quantification of regulatory T cells enables the identification of high-risk breast cancer patients and those at risk of late relapse. J Clin Oncol 24:5373–5380
14. Curiel TJ, Coukos G, Zou L, Alvarez X, Cheng P, Mottram P, Evdemon-Hogan M et al (2004) Specific recruitment of regulatory T cells in ovarian carcinoma fosters immune privilege and predicts reduced survival. Nat Med 10:942–949
15. Perrone G, Ruffini PA, Catalano V, Spino C, Santini D, Muretto P, Spoto C et al (2008) Intratumoural FOXP3-positive regulatory T cells are associated with adverse prognosis in radically resected gastric cancer. Eur J Cancer 44:1875–1882. https://doi.org/10.1016/j.ejca.2008.05.017
16. Hiraoka N, Onozato K, Kosuge T, Hirohashi S (2006) Prevalence of FOXP3+ regulatory Tcells increases during the progression of pancreatic ductal adenocarcinoma and its premalignant lesions. Clin Cancer Res 12:5423–5434
17. Petersen RP, Campa MJ, Sperlazza J, Conlon D, Joshi MB, Harpole DH Jr et al (2006) Tumor infiltrating Foxp3+ regulatory T-cells are associated with recurrence in pathologic stage I NSCLC patients. Cancer 107:2866–2872
18. Panda AK, Bose S, Chakraborty S, Kajal K, Sa G (2015) Intratumoral immune landscape: immunogenicity to tolerogenicity. Austin J Clin Immunol 2:2381–9138
19. Hossain DM, Panda AK, Manna A, Mohanty S, Bhattacharjee P, Bhattacharyya S, Saha T et al (2013) FoxP3 acts as a cotranscription factor with STAT3 in tumor-induced regulatory T cells. Immunity 39:1057–1069. https://doi.org/10.1016/j.immuni.2013.11.005
20. Facciabene A, Motz GT, Coukos G (2012) T-regulatory cells: key players in tumor immune escape and angiogenesis. Cancer Res 72:2162–2171. https://doi.org/10.1158/0008-5472.CAN-11-3687
21. Bergers G, Benjamin LE (2003) Tumorigenesis and the angiogenic switch. Nat Rev Cancer 3:401–410
22. Hanahan D, Weinberg RA (2000) The hallmarks of cancer. Cell 100:57–70
23. Bruno A, Pagani A, Pulze L, Albini A, Dallaglio K, Noonan DM, Mortara L (2014) Orchestration of angiogenesis by immune cells. Front Oncol 4:131. https://doi.org/10.3389/fonc.2014.00131
24. Neufeld G, Cohen T, Gengrinovitch S, Poltorak Z (1999) Vascular endothelial growth factor (VEGF) and its receptors. FASEB J 13:9–22
25. Koch S, Claesson-Welsh L (2012) Signal transduction by vascular endothelial growth factor receptors. Cold Spring Harb Perspect Med. https://doi.org/10.1101/cshperspect.a006502
26. Flow Jo v10 Documentation: tSNE: http://docs.flowjo.com/d2/plugins/tsne/
27. Chakraborty S, Panda AK, Bose S, Roy D, Kajal K, Guha D, Sa G (2017) Transcriptional regulation of FOXP3 requires integrated activation of both promoter and CNS regions in tumor-induced CD8(+) Treg cells. Sci Rep 7:1628. https://doi.org/10.1038/s41598-017-01788-z
28. Kajal K, Panda AK, Bhat J, Chakraborty D, Bose S, Bhattacharjee P, Sarkar T, Chatterjee S, Kar SK, Sa G (2019) Andrographolide binds to ATP-binding pocket of VEGFR2 to impede VEGFA-mediated tumor-angiogenesis. Sci Rep 9(1):4073
29. Sa G, Murugesan G, Jaye M, Ivashchenko Y, Fox PL (1995) Activation of cytosolic phospholipase A2 by basic fibroblast growth factor via a p42 mitogen-activated protein kinase-dependent phosphorylation pathway in endothelial cells. J Biol Chem 270:2360–2366
30. Chakraborty S, Adhikary A, Mazumdar M, Mukherjee S, Bhattacharjee P, Guha D, Choudhuri T et al (2014) Capsaicin-induced activation of p53-SMAR1 auto-regulatory loop down-regulates VEGF in non-small cell lung cancer to restrain angiogenesis. PLoS ONE 9:e99743. https://doi.org/10.1371/journal.pone.0099743
31. Rema RB, Rajendran K, Ragunathan M (2012) Angiogenic efficacy of heparin on chick chorioallantoic membrane. Vasc Cell 4:8. https://doi.org/10.1186/2045-824X-4-8
32. Saha T, Guha D, Manna A, Panda AK, Bhat J, Chatterjee S, Sa G (2016) G-actin guides p53 nuclear transport: potential contribution of monomeric actin in altered localization of mutant p53. Sci Rep 6:32626. https://doi.org/10.1038/srep32626
33. Ray P, Guha D, Chakraborty J, Banerjee S, Adhikary A, Chakraborty S, Das T, Sa G (2016) Crocetin exploits p53-induced death domain (PIDD) and FAS-associated death domain (FADD) proteins to induce apoptosis in colorectal cancer. Sci Rep 6:32979. https://doi.org/10.1038/srep32979

34. Saha S, Mukherjee S, Khan P, Kajal K, Mazumdar M, Manna A, Mukherjee S et al (2016) Aspirin suppresses the acquisition of chemoresistance in breast cancer by disrupting an NFκB-IL6 signaling axis responsible for the generation of cancer stem cells. Cancer Res 76:2000–2012. https://doi.org/10.1158/0008-5472.CAN-15-1360
35. Rabinovich GA, Gabrilovich D, Sotomayor EM (2007) Immunosuppressive strategies that are mediated by tumor cells. Annu Rev Immunol 25:267–296
36. Griffiths RW, Elkord E, Gilham DE, Ramani V, Clarke N, Stern PL, Hawkins RE (2007) Frequency of regulatory T cells in renal cell carcinoma patients and investigation of correlation with survival. Cancer Immunol Immunother 56:1743–1753
37. Jensen HK, Donskov F, Nordsmark M, Marcussen N, von der Maase H (2009) Increased intratumoral FOXP3-positive regulatory immune cells during interleukin-2 treatment in metastatic renal cell carcinoma. Clin Cancer Res 15:1052–1058. https://doi.org/10.1158/1078-0432.CCR-08-1296
38. Gao Q, Qiu SJ, Fan J, Zhou J, Wang XY, Xiao YS, Xu Y et al (2007) Intratumoral balance of regulatory and cytotoxic T cells is associated with prognosis of hepatocellular carcinoma after resection. J Clin Oncol 25:2586–2593
39. Hossain DM, Panda AK, Chakrabarty S, Bhattacharjee P, Kajal K, Mohanty S, Sarkar I et al (2015) MEK inhibition prevents tumour-shed transforming growth factor-beta-induced T-regulatory cell augmentation in tumour milieu. Immunology 144:561–573. https://doi.org/10.1111/imm.12397
40. Jin Y, Liu D, Lin X (2017) IL-35 may maintain homeostasis of the immune microenvironment in periodontitis. Exp Ther Med 14:5605–5610. https://doi.org/10.3892/etm.2017.5255
41. Maaten H (2008) Visualizing data using t-SNE. J Mach Learn Res 9:2579–2605
42. Li X, Gao Y, Li J, Zhang K, Han J, Li W, Hao Q, Zhang W, Wang S, Zeng C, Zhang W, Zhang Y, Li M, Zhang C (2018) FOXP3 inhibits angiogenesis by down regulating VEGF in breast cancer. Cell Death Dis 9(7):744. https://doi.org/10.1038/s41419-018-0790-8